GEOLOGY | THE GEOLOGICAL SOCIETY OF AMERICA®

https://doi.org/10.1130/G47783.1

Manuscript received 20 April 2020
Revised manuscript received 30 July 2020
Manuscript accepted 3 August 2020

Published online 11 September 2020

© 2020 The Authors. Gold Open Access: This paper is published under the terms of the CC-BY license.

Exposure-age data from across Antarctica reveal mid-Miocene establishment of polar desert climate

Perry Spector and Greg Balco
Berkeley Geochronology Center, 2455 Ridge Road, Berkeley, California 94709, USA

ABSTRACT

High-elevation rock surfaces in Antarctica have some of the oldest cosmogenic-nuclide exposure ages on Earth, dating back to the Miocene. A compilation of all available ^{3}He, ^{10}Be, and ^{21}Ne exposure-age data from the Antarctic continent shows that exposure histories recorded by these surfaces extend back to, but not before, the mid-Miocene cooling at 14–15 Ma. At high elevation, this cooling entailed a transition between a climate in which liquid water and biota were present and could contribute to surface weathering and erosion, and a polar desert climate in which virtually all weathering and erosion processes had been shut off. This climate appears to have continued uninterrupted between the mid-Miocene and the present.

INTRODUCTION

From the perspective of Earth's geomorphology, Antarctica is notable because in high-elevation, inland regions, liquid water is almost entirely absent, which leads to a near-total lack of biota and an almost complete standstill of most of the erosional and weathering processes that are active elsewhere on Earth. Marine sedimentary records suggest that this polar desert climate was established during the mid-Miocene cooling ca. 14–15 Ma (e.g., Zachos et al., 2001; Shevenell et al., 2004), and this hypothesis is supported by several lines of evidence from Antarctica, which we summarize below.

Fossil organisms and pollen in terrestrial and marine sediments in Antarctica show that a tundra environment, with mean summer temperatures up to ~5–10 °C, existed during the mid-Miocene and appears to have gone extinct at ca. 14 Ma, replaced by polar conditions that have persisted to the present (Lewis et al., 2008; Ashworth and Cantrill, 2004; Ashworth and Erwin, 2016; Wei et al., 2014; Warny et al., 2009; Anderson et al., 2011). Inland volcanoes in Marie Byrd Land (Fig. 1) show alpine glacial morphology only on pre–mid-Miocene volcanic edifices (Rocchi et al., 2006), and stratigraphic evidence for a shift from wet- to frozen-based glaciation in the Transantarctic Mountains is dated to ca. 14 Ma (Lewis et al., 2008). The evidence from the Transantarctic Mountains implies a cooling of ~8 °C, which is similar to the 6–7 °C cooling estimated for surface waters in the southwestern Pacific Ocean at this time (Shevenell et al., 2004).

Cosmogenic-nuclide exposure dating in Antarctica has established that many rock surfaces currently exposed above the ice sheet have experienced extremely low erosion rates, and therefore that these surfaces record exposure histories that extend millions of years into the past (e.g., Nishiizumi et al., 1991; Van der Wateren et al., 1999; Margerison et al., 2005). Here we exploit a compilation of all available exposure-age data from bedrock and boulder surfaces from Antarctica to show that the exposure history recorded by Antarctic rock surfaces extends back to, but not past, the mid-Miocene cooling at ca. 14–15 Ma. We conclude that this is the result of a transition between a climate in which liquid water and biota were present and could facilitate surface weathering and erosion, and one in which they were absent and could not, and that this condition has been nearly or fully uninterrupted between the mid-Miocene and the present.

CALCULATION OF EXPOSURE AGES

We computed apparent exposure ages from measurements of the stable or long-lived cosmogenic nuclides ^{3}He on pyroxene or olivine, ^{10}Be on quartz, and ^{21}Ne on quartz that are compiled in the ICE-D:ANTARCTICA database (http://antarctica.ice-d.org; Balco, 2020). Apparent exposure ages assume a single, continuous period of exposure during which zero erosion occurs. Hence, for surfaces that have been eroded and/or covered by ice, till, or other material for a portion of their history, apparent exposure ages underestimate true cumulative exposure durations, and thus they are strictly lower limits.

The ICE-D:ANTARCTICA database documents ~3700 samples that were collected for exposure-dating purposes, ~2600 of which have measurements of ^{3}He, ^{10}Be, and/or ^{21}Ne. Of these, 84% are described in at least one of 120 journal articles published between 1986 and 2020 (source references are tabulated at http://antarctica.ice-d.org). The remaining 16% of the samples were nearly all contributed to ICE-D:ANTARCTICA or other public data repositories to satisfy the data dissemination requirements of funding agencies. Samples span the Antarctic continent (Fig. 1), but their distribution is neither random nor systematic, instead reflecting a range of research objectives (from long-term landscape evolution to recent ice-sheet change), the accessibility of field sites, and the interests of individual researchers. Nevertheless, most regions in Antarctica with rock outcrops are represented (Fig. 1).

Production rates and exposure ages for ^{3}He, ^{10}Be, and ^{21}Ne were computed using the production-rate scaling method of Lifton et al. (2014), as implemented in version 3 of the online exposure age calculator described by Balco et al. (2008) and subsequently updated. We used the relationship between Antarctic air pressure and elevation of Stone (2000). Production rates are based on the global calibration data set of Borchers et al. (2016) and ^{21}Ne/^{10}Be production-rate ratios centered on 4.03 (Balco et al., 2019).

DISTRIBUTION OF EXPOSURE AGES IN ANTARCTICA

Extremely old apparent exposure ages of up to 11.1 m.y. (^{3}He), 7.9 m.y. (^{10}Be), and 13.5 m.y. (^{21}Ne) are found at high-elevation

CITATION: Spector, P., and Balco, G., 2020, Exposure-age data from across Antarctica reveal mid-Miocene establishment of polar desert climate: Geology, v. 49, p. 91–95, https://doi.org/10.1130/G47783.1

Downloaded from http://pubs.geoscienceworld.org/gsa/geology/article-pdf/49/1/91/5204761/91.pdf
by guest

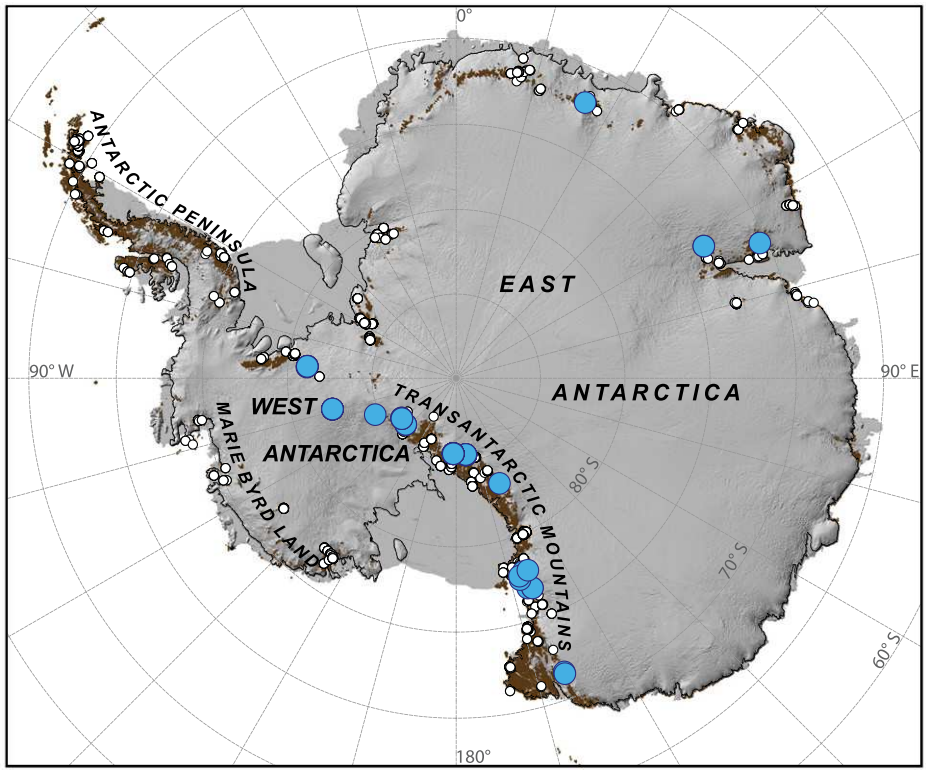

Figure 1. Map of Antarctica showing locations of rock samples in the ICE-D:ANTARCTICA database (http://antarctica.ice-d.org) on which ^{3}He, ^{10}Be, or ^{21}Ne have been measured (white circles). Blue circles show samples with Miocene exposure ages older than 5.3 Ma. Areas with rock outcroppings are shown in brown.

sites in Antarctica (Fig. 2; see the Supplemental Material[1]). While ^{3}He and ^{21}Ne are stable nuclides, ^{10}Be is radioactive with a 1.4 m.y. half-life. After ~7 m.y. (5 half-lives) of continuous exposure and zero erosion, ^{10}Be concentrations asymptotically approach a "saturated" steady state such that nuclide production is balanced by radioactive decay. Thus, samples with apparent ^{10}Be exposure ages of ~7–8 m.y. may, in fact, have experienced much longer exposure histories.

The oldest samples in our compilation were collected from high-elevation sites in the Transantarctic Mountains or from isolated nunataks in East and West Antarctica (Figs. 1 and 3C). These sites experience a climate that is perennially extremely cold and arid and thus are nearly completely devoid of liquid water and biota (Graly et al., 2018; Dragone and Fierer, 2019). The high-elevation regions where these sites are located are also where glacier and ice-sheet velocities are lowest, ice (where present) is frozen to the bed, and ice thickening during

[1]Supplemental Material. Table S1 (sample and exposure-age information for all samples in the ICE-D:ANTARCTICA database that have Miocene apparent exposure ages). Please visit https://doi.org/10.1130/GEOL.S.12869681 to access the supplemental material, and contact editing@geosociety.org with any questions.

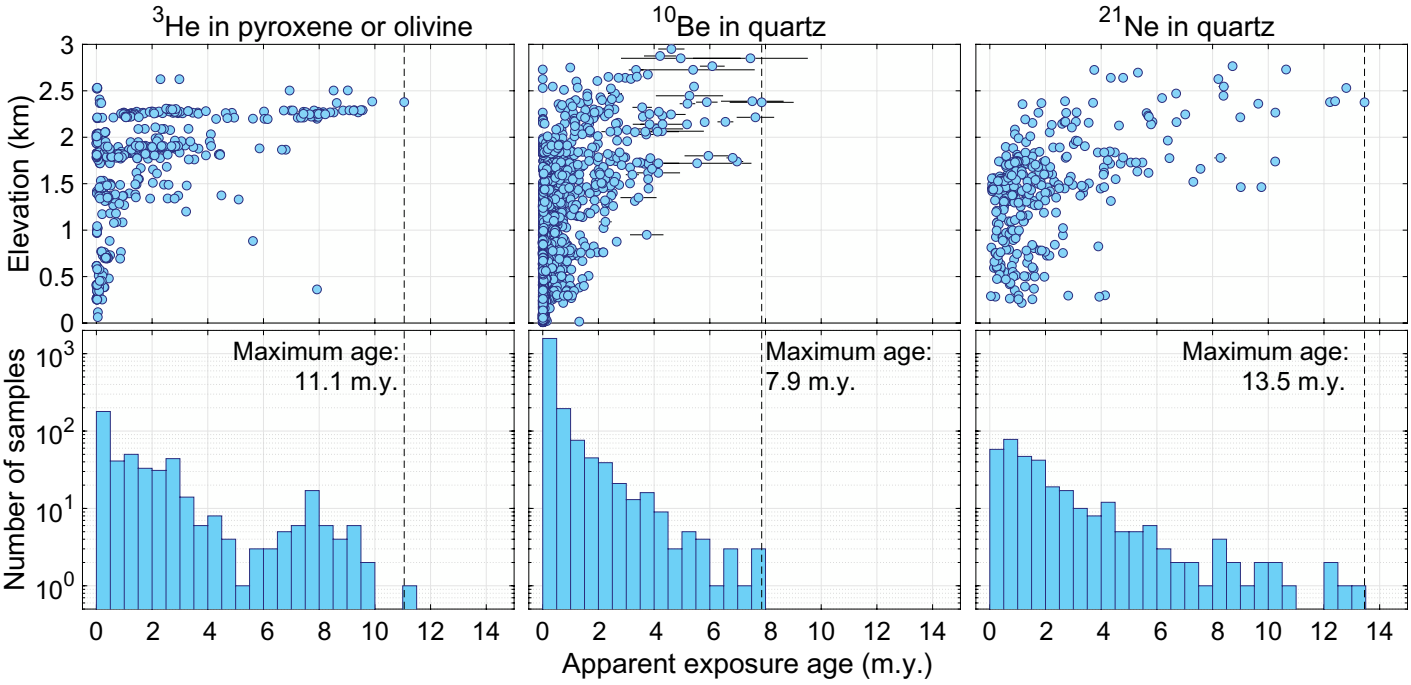

Figure 2. Upper panels show relationship between elevation and apparent exposure age for all rock samples in the ICE-D:ANTARCTICA database (http://antarctica.ice-d.org) with measurements of ^{3}He in pyroxene or olivine, ^{10}Be in quartz, and ^{21}Ne in quartz. Error bars represent 68% confidence intervals. Lower panels show log-scaled histograms of apparent exposure ages for these nuclides. Dashed lines indicate the oldest age in each population. We are unable to compute exposure ages with finite uncertainties for five samples that are saturated with respect to ^{10}Be, and thus these samples are not represented in this figure.

Downloaded from http://pubs.geoscienceworld.org/gsa/geology/article-pdf/49/1/91/5204761/91.pdf
by guest

Figure 3. Examples of young and ancient Antarctic rock surfaces. (A) Frost-shattered bedrock at an elevation of 520 m on Downham Peak, which lies outboard of the present-day grounding line in the Antarctic Peninsula. This site is likely ice-covered only for short periods at glacial maxima, so its apparent exposure age of 26 ka implies relatively rapid surface weathering in this coastal environment (Balco et al., 2013). (B) Striated granite at an elevation of 100–200 m on Mount Hope in the central Transantarctic Mountains (photo by John Stone). View is looking up the Beardmore Glacier, which covered this site during the last ice age. (C) Oxidized granite surface at an elevation of 2350 m on Mount Seelig in the Whitmore Mountains, which are located on the divide of the West Antarctic Ice Sheet (photo by John Stone). Sample bag shows location of sample 13-NTK-040-WHT, which has an apparent ^{21}Ne age of ~10 m.y. (Spector, 2018). Sample bags in panels A and C are ~30 cm in length.

past glacial periods was limited (Spector et al., 2019). As a result of these meteorological and glaciological factors, nearly all weathering, erosion, and sediment transport processes, both subaerial and subglacial, do not operate in these regions at present, and have likely been minimal throughout the Quaternary.

In contrast, samples located below ~1000 m elevation have young exposure ages, ranging from Holocene on deposits emplaced during the most recent deglaciation to early and middle Pleistocene on various older deposits and bedrock surfaces (Fig. 2). Due to the parabolic profile of the ice sheet, low-elevation ice-free areas in Antarctica are found only near the coastal perimeter. Low elevation and proximity to the ocean imply the highest temperature and precipitation in the continent, so rock surface weathering rates are relatively high (Fig. 3A). Low-elevation ice-marginal sites are also both adjacent to fast-flowing outlet glaciers and subject to the largest glacial-interglacial changes in ice thickness, factors that increase the likelihood of subglacial erosion by wet-based ice during glacial periods (e.g., Sugden et al., 2005; Fig. 3B). For example, two of the warmest and wettest regions in Antarctica are the Antarctic Peninsula and Marie Byrd Land (Fig. 1). These regions are represented by ~10% of the samples in our analysis, but none of these samples have an exposure age exceeding 1 m.y.

Apparent exposure ages alone show that the oldest sample in our compilation has been exposed for at least 13.5 m.y., and that several samples have been exposed for at least 11 m.y. We hypothesize that preservation and exposure of these high-elevation rock surfaces at near-zero erosion rates began during the mid-Miocene cooling at 14–15 Ma. Prior to that time, the Antarctic climate was warmer (Lewis and Ashworth, 2016), which, by analogy to Arctic mountain ranges where water and biota are present (see discussion below), resulted in much higher weathering and erosion rates.

EFFECT OF SLOW SURFACE EROSION ON EXPOSURE AGES

Erosion reduces apparent exposure ages by removing the outer layer of rock, which has received the highest cosmic-ray dose (Lal, 1988). Our objective here is to determine whether the oldest samples from Antarctica are consistent with continuous exposure for the past 14–15 m.y. at very low erosion rates, or whether much older exposure durations are permitted, which would falsify our hypothesis. To quantify this, we rely on samples on which both ^{10}Be and ^{21}Ne have been measured. Measurements of two nuclides with different decay rates can constrain two unknown values related to the geomorphic history of a sample, and in this case, we solve simultaneously for the exposure age and the steady erosion rate (Lal, 1991; Fig. 4).

The paired-nuclide data (Fig. 4) show that although the oldest samples have apparent ^{21}Ne exposure ages (assuming zero erosion) up to 13.5 m.y., three samples are consistent

Downloaded from http://pubs.geoscienceworld.org/gsa/geology/article-pdf/49/1/91/5204761/91.pdf
by guest

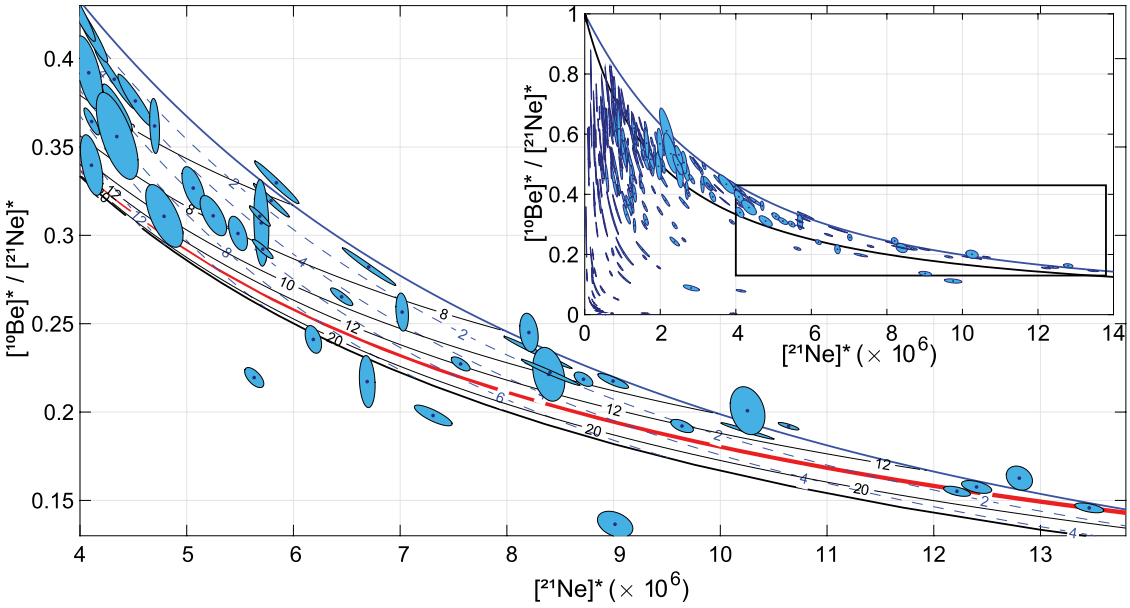

Figure 4. ^{10}Be-^{21}Ne diagram for all rock samples on which both nuclides have been measured (*n* = 261). Asterisks indicate that nuclide concentrations are normalized to the surface production rates for each sample. The abscissa is equivalent to the apparent ^{21}Ne exposure age, and thus is a lower bound on true cumulative exposure. Ellipses represent 68% confidence regions. Nuclide concentrations of continuously exposed, non-eroding samples would lie along the upper blue line ("simple-exposure line"). Nuclide concentrations of samples that have reached production-decay-erosion equilibrium would plot along the lower black line ("steady-erosion line"). These lines bound the "simple-exposure region". Main panel expands the area in the rectangle in the upper-right panel. The simple-exposure region in the main panel is contoured with dashed blue isolines of erosion rate (in cm m.y.$^{-1}$) and solid black isolines of exposure age (in m.y.). Red band represents the 14–15 m.y. exposure-age contour. All Miocene-age samples that lie in the simple-exposure region plot along or above the 14–15 m.y. contour band (i.e., they are younger than ~15 m.y.) and are thus consistent with the hypothesis that no rock surface in Antarctica has an exposure age that pre-dates the mid-Miocene climate transition. Miocene-age samples that lie below the simple-exposure region reflect past ice-sheet cover and/or non-steady erosion.

with 14–15 m.y. of continuous exposure at extremely low erosion rates of <2 cm m.y.$^{-1}$. Although unrecognized past ice cover of these samples would cause us to slightly overestimate the true erosion rates and exposure ages, these samples lie near the simple-exposure line and thus require near-continuous exposure. Our hypothesis predicts that no sample should have an exposure age >14–15 m.y., and this is, in fact, what we observed. All old samples that lie within the simple-exposure region are consistent with exposure ages indistinguishable from, or postdating, the mid-Miocene climate transition at 14–15 Ma.

In addition to surface erosion, surface uplift can cause the apparent exposure age of a rock surface to underestimate the true age. Peaks in some areas of Antarctica are hypothesized to experience uplift on million-year time scales due to isostatic compensation of bedrock erosion beneath nearby outlet glaciers (e.g., Stern et al., 2005; Sugden et al., 2014) or time-varying dynamic topography (Austermann et al., 2015). From the perspective of a rock surface, uplift and erosion are the same: both cause the production rate to increase over time by removing overlying mass—atmosphere for uplift, rock for erosion—that previously shielded the surface from the cosmic-ray flux. An uplift constraint can therefore be substituted for an erosion constraint (Balter et al., 2020). If we assume a limiting case of zero erosion for the oldest surfaces, their nuclide concentrations are consistent with uplift rates of ~35–40 m m.y.$^{-1}$. Although Figure 4 is drawn under the assumption that surfaces are experiencing erosion and not uplift, the uplift-erosion equivalency means that this assumption does not affect the exposure-age constraints inferred from the paired-nuclide data.

EROSION RATES REMAINED LOW DURING WARM CLIMATES

Marine sediment records and climate-model experiments suggest that portions of Antarctica were 5–10 °C warmer during the late Miocene and Pliocene than during the pre-industrial period (Zachos et al., 2001; DeConto and Pollard, 2016; Herbert et al., 2016). Liquid water and biota may have been more abundant at these times, so rock weathering and erosion rates may have been elevated. The closest analogue to the late Miocene and Pliocene climates of Antarctica may be the Pleistocene Arctic, where the highest measured cosmogenic-nuclide concentrations in rock surfaces record no more than ~1 m.y. of exposure and imply erosion rates >50 cm m.y.$^{-1}$ (Margreth et al., 2016; Strunk et al., 2017). Although the oldest Antarctic surfaces indicate much lower erosion rates (Fig. 4), some are consistent with a scenario in which erosion rates were somewhat higher during past warm periods.

To quantify this, we calculated the maximum duration that Antarctic rock surfaces could have eroded at 50 cm m.y.$^{-1}$—the lowest rate implied by Arctic rock surfaces—during the late Miocene and Pliocene. The most restrictive constraints come from samples that are at or near saturation with respect to ^{10}Be. An upper limit on the duration of accelerated erosion is obtained by assuming a scenario in which ^{10}Be concentrations were initially at saturation, decreased during a period in which rock surfaces eroded at 50 cm m.y.$^{-1}$, and subsequently increased to present-day values under zero erosion. If we assume that erosion occurred at ca. 3 Ma during the Pliocene, then samples with present-day ^{10}Be concentrations near saturation permit erosion for no more than ~80 k.y. Longer erosion durations are permissible if they occurred earlier during the late Miocene, for example, ~250 k.y. of erosion at ca. 5 Ma.

Even with the conservative assumption of initial ^{10}Be saturation, these results indicate that Antarctic erosion rates during warm climates of the late Miocene and Pliocene rarely, if ever, approached even the lowest Pleistocene erosion rates implied by Arctic rock surfaces. Therefore, we surmise that at high-elevation sites in Antarctica, polar desert conditions have persisted with zero or minimal interruption since the mid-Miocene cooling at 14–15 Ma.

SUMMARY

The oldest rock surfaces in Antarctica have been continuously exposed for 14–15 m.y. at extraordinarily slow erosion rates of 2 cm m.y.$^{-1}$ or less. Of the ~2600 samples in our compilation, none indicate exposure for more than 14–15 m.y. Samples that are at or near saturation with respect to ^{10}Be require that erosion rates remained very low for the vast majority of the late Miocene

Downloaded from http://pubs.geoscienceworld.org/gsa/geology/article-pdf/49/1/91/5204761/91.pdf
by guest

and Pliocene, periods when it is presumed that Antarctica experienced a warmer-than-present climate. Hence all exposure-age data from high-elevation, inland sites support the hypothesis that the mid-Miocene cooling at 14–15 Ma resulted in a polar desert climate that shut down virtually all weathering and erosion processes, and that this climate appears to have persisted with zero or minimal interruption to the present.

ACKNOWLEDGMENTS

Support for this work was provided by the Ann and Gordon Getty Foundation (San Francisco, California, USA) and by the U.S. National Science Foundation under grant OPP-1744771. We thank David Sugden, David Fink, and an anonymous reviewer for constructive feedback that improved the manuscript.

REFERENCES CITED

Anderson, J.B., et al., 2011, Progressive Cenozoic cooling and the demise of Antarctica's last refugium: Proceedings of the National Academy of Sciences of the United States of America, v. 108, p. 11,356–11,360, https://doi.org/10.1073/pnas.1014885108.

Ashworth, A.C., and Cantrill, D.J., 2004, Neogene vegetation of the Meyer Desert Formation (Sirius Group) Transantarctic Mountains, Antarctica: Palaeogeography, Palaeoclimatology, Palaeoecology, v. 213, p. 65–82, https://doi.org/10.1016/S0031-0182(04)00359-1.

Ashworth, A.C., and Erwin, T.L., 2016, *Antarctotrechus balli* sp. n. (Carabidae, Trechini): The first ground beetle from Antarctica: ZooKeys, no. 635, p. 109–122, https://doi.org/10.3897/zookeys.635.10535.

Austermann, J., Pollard, D., Mitrovica, J.X., Moucha, R., Forte, A.M., DeConto, R.M., Rowley, D.B., and Raymo, M.E., 2015, The impact of dynamic topography change on Antarctic ice sheet stability during the mid-Pliocene warm period: Geology, v. 43, p. 927–930, https://doi.org/10.1130/G36988.1.

Balco, G., 2020, Technical note: A prototype transparent-middle-layer data management and analysis infrastructure for cosmogenic-nuclide exposure dating: Geochronology, v. 2, p. 169–175, https://doi.org/10.5194/gchron-2-169-2020.

Balco, G., Stone, J.O., Lifton, N.A., and Dunai, T.J., 2008, A complete and easily accessible means of calculating surface exposure ages or erosion rates from ^{10}Be and ^{26}Al measurements: Quaternary Geochronology, v. 3, p. 174–195, https://doi.org/10.1016/j.quageo.2007.12.001.

Balco, G., Schaefer, J.M., and LARISSA Group, 2013, Exposure-age record of Holocene ice sheet and ice shelf change in the northeast Antarctic Peninsula: Quaternary Science Reviews, v. 59, p. 101–111, https://doi.org/10.1016/j.quascirev.2012.10.022.

Balco, G., Blard, P.-H., Shuster, D.L., Stone, J.O.H., and Zimmermann, L., 2019, Cosmogenic and nucleogenic ^{21}Ne in quartz in a 28-meter sandstone core from the McMurdo Dry Valleys, Antarctica: Quaternary Geochronology, v. 52, p. 63–76, https://doi.org/10.1016/j.quageo.2019.02.006.

Balter, A., Bromley, G., Balco, G., Thomas, H., and Jackson, M.S., 2020, A 14.5 million-year record of East Antarctic Ice Sheet fluctuations from the central Transantarctic Mountains, constrained with cosmogenic ^{3}He, ^{10}Be, ^{21}Ne, and ^{26}Al: The Cryosphere, https://doi.org/10.5194/tc-2020-57 (in press).

Borchers, B., Marrero, S., Balco, G., Caffee, M., Goehring, B., Lifton, N., Nishiizumi, K., Phillips, F., Schaefer, J., and Stone, J., 2016, Geological calibration of spallation production rates in the CRONUS-Earth project: Quaternary Geochronology, v. 31, p. 188–198, https://doi.org/10.1016/j.quageo.2015.01.009.

DeConto, R.M., and Pollard, D., 2016, Contribution of Antarctica to past and future sea-level rise: Nature, v. 531, p. 591–597, https://doi.org/10.1038/nature17145.

Dragone, N., and Fierer, N., 2019, Identification of uninhabited surface soils in the Shackleton Glacier Valley: Abstract presented at the 4th Interdisciplinary Antarctic Earth Sciences Conference, Julian, California, 13–15 October.

Graly, J.A., Licht, K.J., Druschel, G.K., and Kaplan, M.R., 2018, Polar desert chronologies through quantitative measurements of salt accumulation: Geology, v. 46, p. 351–354, https://doi.org/10.1130/G39650.1.

Herbert, T.D., Lawrence, K.T., Tzanova, A., Peterson, L.C., Caballero-Gill, R., and Kelly, C.S., 2016, Late Miocene global cooling and the rise of modern ecosystems: Nature Geoscience, v. 9, p. 843–847, https://doi.org/10.1038/ngeo2813.

Lal, D., 1988, In situ–produced cosmogenic isotopes in terrestrial rocks: Annual Review of Earth and Planetary Sciences, v. 16, p. 355–388, https://doi.org/10.1146/annurev.ea.16.050188.002035.

Lal, D., 1991, Cosmic ray labeling of erosion surfaces: In situ nuclide production: Earth and Planetary Science Letters, v. 104, p. 424–439, https://doi.org/10.1016/0012-821X(91)90220-C.

Lewis, A.R., and Ashworth, A.C., 2016, An early to middle Miocene record of ice-sheet and landscape evolution from the Friis Hills, Antarctica: Geological Society of America Bulletin, v. 128, p. 719–738, https://doi.org/10.1130/B31319.1.

Lewis, A.R., et al., 2008, Mid-Miocene cooling and the extinction of tundra in continental Antarctica: Proceedings of the National Academy of Sciences of the United States of America, v. 105, p. 10,676–10,680, https://doi.org/10.1073/pnas.0802501105.

Lifton, N., Sato, T., and Dunai, T.J., 2014, Scaling in situ cosmogenic nuclide production rates using analytical approximations to atmospheric cosmic-ray fluxes: Earth and Planetary Science Letters, v. 386, p. 149–160, https://doi.org/10.1016/j.epsl.2013.10.052.

Margerison, H.R., Phillips, W.M., Stuart, F.M., and Sugden, D.E., 2005, Cosmogenic ^{3}He concentrations in ancient flood deposits from the Coombs Hills, northern Dry Valleys, East Antarctica: Interpreting exposure ages and erosion rates: Earth and Planetary Science Letters, v. 230, p. 163–175, https://doi.org/10.1016/j.epsl.2004.11.007.

Margreth, A., Gosse, J.C., and Dyke, A.S., 2016, Quantification of subaerial and episodic subglacial erosion rates on high latitude upland plateaus: Cumberland Peninsula, Baffin Island, Arctic Canada: Quaternary Science Reviews, v. 133, p. 108–129, https://doi.org/10.1016/j.quascirev.2015.12.017.

Nishiizumi, K., Kohl, C.P., Arnold, J.R., Klein, J., Fink, D., and Middleton, R., 1991, Cosmic ray produced ^{10}Be and ^{26}Al in Antarctic rocks: Exposure and erosion history: Earth and Planetary Science Letters, v. 104, p. 440–454, https://doi.org/10.1016/0012-821X(91)90221-3.

Rocchi, S., LeMasurier, W.E., and Di Vincenzo, G., 2006, Oligocene to Holocene erosion and glacial history in Marie Byrd Land, West Antarctica, inferred from exhumation of the Dorrel Rock intrusive complex and from volcano morphologies: Geological Society of America Bulletin, v. 118, p. 991–1005, https://doi.org/10.1130/B25675.1.

Shevenell, A.E., Kennett, J.P., and Lea, D.W., 2004, Middle Miocene Southern Ocean cooling and Antarctic cryosphere expansion: Science, v. 305, p. 1766–1770, https://doi.org/10.1126/science.1100061.

Spector, P., 2018, Antarctic glacial history inferred from cosmogenic-nuclide measurements in rocks [Ph.D. thesis]: Seattle, University of Washington, 118 p.

Spector, P., Stone, J., and Goehring, B., 2019, Thickness of the divide and flank of the West Antarctic Ice Sheet through the last deglaciation: The Cryosphere, v. 13, p. 3061–3075, https://doi.org/10.5194/tc-13-3061-2019.

Stern, T.A., Baxter, A.K., and Barrett, P.J., 2005, Isostatic rebound due to glacial erosion within the Transantarctic Mountains: Geology, v. 33, p. 221–224, https://doi.org/10.1130/G21068.1.

Stone, J.O., 2000, Air pressure and cosmogenic isotope production: Journal of Geophysical Research, v. 105, p. 23,753–23,759, https://doi.org/10.1029/2000JB900181.

Strunk, A., Knudsen, M.F., Egholm, D.L., Jansen, J.D., Levy, L.B., Jacobsen, B.H., and Larsen, N.K., 2017, One million years of glaciation and denudation history in west Greenland: Nature Communications, v. 8, 14199, https://doi.org/10.1038/ncomms14199.

Sugden, D.E., Balco, G., Cowdery, S.G., Stone, J.O., and Sass, L.C., III, 2005, Selective glacial erosion and weathering zones in the coastal mountains of Marie Byrd Land, Antarctica: Geomorphology, v. 67, p. 317–334, https://doi.org/10.1016/j.geomorph.2004.10.007.

Sugden, D.E., Fogwill, C.J., Hein, A.S., Stuart, F.M., Kerr, A.R., and Kubik, P.W., 2014, Emergence of the Shackleton Range from beneath the Antarctic Ice Sheet due to glacial erosion: Geomorphology, v. 208, p. 190–199, https://doi.org/10.1016/j.geomorph.2013.12.004.

Van der Wateren, F.M., Dunai, T.J., Van Balen, R.T., Klas, W., Verbers, A.L.L.M., Passchier, S., and Herpers, U., 1999, Contrasting Neogene denudation histories of different structural regions in the Transantarctic Mountains rift flank constrained by cosmogenic isotope measurements: Global and Planetary Change, v. 23, p. 145–172, https://doi.org/10.1016/S0921-8181(99)00055-7.

Warny, S., Askin, R.A., Hannah, M.J., Mohr, B.A., Raine, J.I., Harwood, D.M., Florindo, F., and SMS Science Team, 2009, Palynomorphs from a sediment core reveal a sudden remarkably warm Antarctica during the middle Miocene: Geology, v. 37, p. 955–958, https://doi.org/10.1130/G30139A.1.

Wei, L.J., Raine, J.I., and Liu, X.H., 2014, Terrestrial palynomorphs of the Cenozoic Pagodroma Group, northern Prince Charles Mountains, East Antarctica: Antarctic Science, v. 26, p. 69–79, https://doi.org/10.1017/S0954102013000278.

Zachos, J., Pagani, M., Sloan, L., Thomas, E., and Billups, K., 2001, Trends, rhythms, and aberrations in global climate 65 Ma to present: Science, v. 292, p. 686–693, https://doi.org/10.1126/science.1059412.

Printed in USA

Downloaded from http://pubs.geoscienceworld.org/gsa/geology/article-pdf/49/1/91/5204761/91.pdf
by guest